THE JOURNAL OF PHYSICAL CHEMISTRY A

Article

pubs.acs.org/JPCA

Controlling Dissociation of Alkyl Phenyl Ketone Radical Cations in the Strong-Field Regime through Hydroxyl Substitution Position

Katharine Moore Tibbetts, Timothy Bohinski, Kristin Munkerup, Maryam Tarazkar, and Robert Levis*

Center for Advanced Photonics Research and Department of Chemistry, Temple University, Philadelphia, Pennsylvania 19122, United States

ABSTRACT: The hydroxy-substituted alkyl phenyl ketones 2′-, 3′- and 4′- (ortho, meta, and para) hydroxyacetophenone were excited in the strong-field regime with wavelengths ranging from 1200−1500 nm to produce the respective radical cations. For 2′- and 3′-hydroxyacetophenone, the parent molecular ion dominated the mass spectrum, and the intensity of the fragment ions remained unchanged as a function of excitation wavelength. In contrast, 4′-hydroxyacetophenone exhibited depletion of the parent molecular ion with corresponding enhanced formation of the benzoyl fragment ion upon excitation with 1370 nm as compared with other excitation wavelengths. Density functional (DFT) calculations suggest that dissociation occurs when the acetyl group in 4′-hydroxyacetophenone radical cation twists out-of-plane with respect to the phenyl ring, enabling a one-photon transition between the ground cation state D_0 and the excited cation state D_2 to occur. The DFT calculations also suggest that the lack of dissociation in the wavelength-resolved strong-field excitation measurements for 2′- and 3′-hydroxyacetophenone arises because both isomers have a barrier to rotation about the carbon−carbon bond connecting the phenyl and acetyl groups. These results help elucidate the effects of substituents on the torsional motion of radical cations and illustrate the potential for controlling molecular dissociation through the addition of substituents.

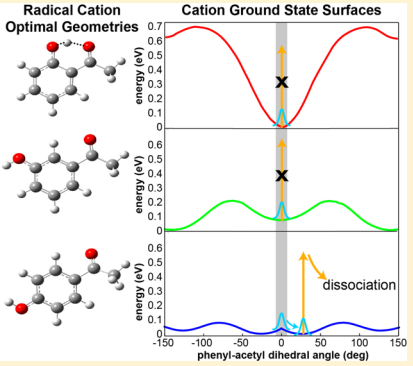

INTRODUCTION

A central goal in chemistry is to understand and manipulate molecular properties through the addition of chemical substituents at particular sites on the molecule.[1−3] Recently, strong-field ionization and mass spectrometry have been employed to assess the effects of substituent groups on molecular properties such as cationic excited state energies, vibrational couplings, and dissociation dynamics.[4−9] In fluoro- and methoxy-substituted phenols, the substitution pattern on the phenyl ring was found to determine the adiabatic ionization energy and vibrational energy levels.[5] Time-resolved experiments and quantum calculations for trifluoroacetone and trichloroacetone revealed enhanced dissociation when the delay between the pump and probe pulses matched the vibrational dynamics of the respective molecules, with the longer vibrational period of trichloroacetone correlating with a longer time delay producing the maximum fragmentation yield.[6] Time-resolved studies of halogenated organometallic compounds $CpFe(CO)_2X$ (X = Cl, Br, I) revealed an inverse correlation between the halogen size and time required for dissociation of both CO ligands from the compound. This trend was attributed to the more efficient overlap of the chlorine orbitals with the metal center in comparison with those of the larger atoms bromine and iodine.[7] The relative yields of halogen ions from halomethanes (CH_2XY, X, Y = F, Cl, Br, I) have also been found to increase systematically as a function of halogen size upon interaction with families of ultrafast laser pulses with phase shaping using an adaptive genetic algorithm[9] and varying polynomial spectral phase.[8,10] In these studies, the increased halogen ion yields from bromine- and iodine-containing molecules were attributed to their lower ionization potentials.

The multiphoton ionization processes occurring in strong-field photodissociation/ionization experiments using 800 nm, and shorter, laser wavelengths can make mechanistic interpretation of substituent effects in larger polyatomic systems difficult. The mechanism may be obscured by the population of multiple vibronic states in the cation, and such excited states often result in a high degree of molecular dissociation through various pathways.[11] In contrast, ionizing with longer wavelengths (e.g., in the near-infrared) allows an electron to tunnel through the potential barrier, leaving the cation in the ground electronic state with little vibrational excitation, and this adiabatic ionization typically decreases fragmentation.[11] The tunnel ionization mechanism produces a ground ionic "launch" state in the radical cation that can be further excited to probe the low-lying cationic energy states, thus enabling more straightforward interpretation of the resulting fragmentation dynamics.

Strong-field tunnel ionization/dissociation measurements using wavelengths ranging from 1200 to 1500 nm have recently been used to probe the low-lying cationic electronic states of acetophenone, propiophenone, and related methyl-substituted derivatives.[11,12] Because of adiabatic ionization conditions, the

Special Issue: A. W. Castleman, Jr. Festschrift

Received: January 24, 2014
Revised: February 25, 2014

   dx.doi.org/10.1021/jp500874r | J. Phys. Chem. A XXXX, XXX, XXX−XXX

Table 1. Energies, Angles, and Bond Lengths of the Radical Cations of 2′-, 3′-, and 4′-Hydroxyacetophenone: Experimental Vertical Ionization Potentials (IP_{exp}),[18−20] Calculated Values of Vertical Ionization Potentials (IP_{calc}), the Energy Difference ($E_{neut\text{-}opt}$), and Change in O−H Bond Length ($D(OH)_{neut\text{-}opt}$) between the Neutral Vertical Geometry and the Optimized Geometry on the Cationic Ground-State Surface, the Dihedral Angle in the Optimized Radical Cations, and the Reduced Moments of Inertia in Atomic Units[a]

	2′-hydroxyacetophenone	3′-hydroxyacetophenone	4′-hydroxyacetophenone	acetophenone
IP_{exp} (eV)	N/A	8.67	8.70	9.28
IP_{calc} (eV)	8.59	8.74	8.72	9.32
$E_{neut\text{-}opt}$ (eV)	0.22	0.22	0.26	0.31
$D(OH)_{neut\text{-}opt}$ (Å)	0.047	0.010	0.007	N/A
phenyl-acetyl dihedral angle (deg)	0	5	35	44
reduced moment of inertia (a.u.)	128.65	127.07	112.42	111.46

[a]Calculations for acetophenone were performed at the EOM-IP-CCSD/6-311+G(d) level of theory.[11]

parent molecular ion is typically the dominant photoproduct in the mass spectrum using near-infrared excitation wavelengths. However, upon ionization of acetophenone with 1370 nm, a significant depletion of the parent ion yield was observed, accompanied by an increased yield of the benzoyl photoproduct (corresponding to the loss of the methyl group). This enhanced dissociation feature in the mass spectral response at 1370 nm was observed only for molecules containing both the phenyl and carbonyl groups; the response of the homologues ethyl benzene and acetone was featureless.[11] The enhanced benzoyl ion production was found to arise from a resonant one-photon transition between the cationic ground-state D_0 and the excited-state D_2. Calculations revealed that the transition becomes allowed following torsional motion about the phenyl−acetyl carbon−carbon bond.

Methyl-substituted acetophenones were recently observed to possess a similar resonant dissociation feature, where the degree of parent ion depletion upon 1370 nm excitation increased as the position of the methyl group on the phenyl ring was moved from ortho to meta to para with respect to the acetyl moiety.[12] 4′-Methylacetophenone had a spectrally resolved parent ion depletion feature that was virtually identical to the acetophenone measurements.[11] Calculations at the B3LYP/6-311++G(d,p) level of theory for 2′-methylacetophenone indicated that a favorable interaction between a hydrogen atom from the ortho methyl group and the carbonyl oxygen hindered the torsional motion about the phenyl−acetyl carbon−carbon bond. The larger moments of inertia for 2′- and 3′-methylacetophenone also slowed the torsional motion to the bright geometry within the duration of the laser pulse as compared with the 4′-methylacetophenone.[12]

We investigate fragmentation yields in the family of hydroxy-substituted alkyl phenyl ketones: 2′-, 3′-, and 4′-hydroxyacetophenone. Mass spectra are recorded as a function of strong-field excitation wavelength ranging from 1200−1500 nm. Electronic structure calculations are performed on the molecules to determine the nuclear configurations corresponding to the energy minima of the neutral molecules and radical cations as well as to map out the cationic ground-state potential energy surfaces along the phenyl−acetyl torsional coordinate. The experimental results are explained in terms of calculated potential-energy surfaces of the ground ionic states of each isomer.

EXPERIMENTAL SECTION

The experimental setup used to perform radical cation spectroscopy has been previously described.[11,13] In brief, a Ti:sapphire amplifier pumps an optical parametric amplifier (OPA) to generate tunable signal IR pulses from 1150 to 1550 nm with pulse durations from 50 to 120 fs. Pulse durations for the following experiments were determined by frequency-resolved optical gating and maintained at either 65 ± 5 or 110 ± 5 fs across the tuning range. The excitation beam was focused by a plano-convex lens with f = 20 cm to reach intensities ranging between 2.0 and 8.0 × 10^{13} W cm^{-2} in the extraction region of a time-of flight mass spectrometer (TOF-MS) with a base pressure 1.3 × 10^{-6} Pa. The pulse energy was attenuated using a circular variable neutral density filter. Samples of 2′-, 3′-, and 4′-hydroxyacetophenone (Sigma Aldrich) were used without further purification and leaked into the vacuum chamber via a variable leak valve to obtain a pressure of 4.8 × 10^{-4} Pa. The sample holder was heated to 35 °C to increase the vapor pressure sufficiently such that an appreciable signal from 3′- and 4′-hydroxyacetopheone could be obtained. The laser intensity was internally calibrated[14] at each wavelength by measuring the xenon ion yield introduced using a second leak valve, with an estimated error of ±2 × 10^{12} W cm^{-2}.

Calculations. Electronic structure calculations using density functional theory (DFT) were performed using the Gaussian09 program package.[15] The B3LYP/6-311++G(d,p) level of theory was used for all geometry optimizations. The same level of theory was employed to calculate the ground state potential energy surfaces of the 2′-, 3′-, and 4′-hydroxyacetophenone radical cations as a function of the angle of the phenyl-acetyl torsional coordinate. Although density functional methods are suitable for calculating the ground state energy of radical cations because they minimize the effects of spin contamination compared to Hartree−Fock methods, the exchange correlation energy must be approximated.[16,17] The B3LYP basis set used in this study is a hybrid functional that includes a fraction of the Hartree−Fock exchange correlation energy. The resulting error in the potential energy surfaces is expected to be ∼0.1 eV based on the error between the experimental and calculated values of the ionization potentials reported in Table 1.

RESULTS

Figure 1 shows the mass spectra of 2′-, 3′-, and 4′-hydroxyacetophenone upon ionization with 65 fs pulses at 1200 (a−c) and 1370 nm (d−f) at an intensity of 5.5 × 10^{13} W cm^{-2}. At 1200 nm, the parent molecular ion is the major peak in the mass spectrum, and little fragmentation is observed, suggesting that tunnel ionization is the dominant mechanism. Ionizing these molecules with 800 nm was found to produce significantly higher yields of small mass fragments below m/z = 93 (not shown), consistent with multiphoton ionization excitation to high-lying electronic states that leads to multiple

dx.doi.org/10.1021/jp500874r | J. Phys. Chem. A XXXX, XXX, XXX−XXX

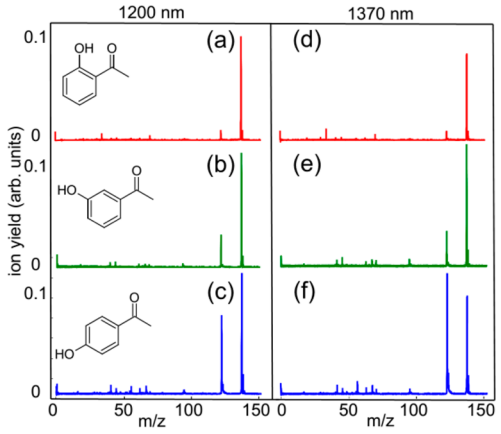

Figure 1. TOF spectra of 2′-hydroxyacetophenone ((a,d) red), 3′-hydroxyacetophenone ((b,e) green), and 4′-hydroxyacetophenone ((c,f) blue) using an excitation wavelength of 1200 (a–c) and 1370 nm (d–f). The laser intensity was 5.5 × 10^{13} W cm^{-2}, and the pulse duration was 65 fs.

dissociation channels, as seen in related studies.[12,13] At 1370 nm excitation, the parent molecular ion is still the major peak in the mass spectra of 2′- and 3′-hydroxyacetophenone. In contrast, the benzoyl ion is the major peak in the spectrum of 4′-hydroxyacetophenone excited with 1370 nm, while the parent ion yield is depleted. This behavior is consistent with that of acetophenone and its derivatives,[11,12] where the benzoyl formation is attributed to a one-photon excitation from the ground cationic state D_0 to the second cationic excited state D_2. For all isomers, the mass spectral patterns do not change significantly as a function of laser intensity at a given excitation wavelength. The yields of each ion increase linearly with intensity at all excitation wavelengths, as shown in Figure 2 for the parent and benzoyl ion from 2′-hydroxyacetophenone using excitation at 1260 nm; the other isomers exhibited similar behavior.

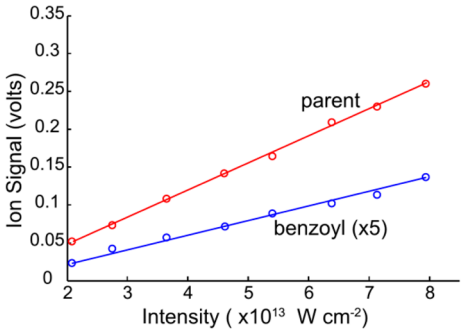

Figure 2. Ion yield of parent molecular ion (red) and benzoyl ion (blue) from 2′-hydroxyacetophenone as a function of laser intensity at 1260 nm. The benzoyl ion is magnified five times for ease of comparison. The pulse duration was 65 fs.

The normalized yields of the parent and benzoyl ions upon excitation with 1200–1500 nm are plotted in Figure 3 for (a) 2′-, (b) 3′-, and (c) 4′-hydroxyacetophenone at a laser intensity of ~5.5 × 10^{13} W cm^{-2} and pulse duration of 65 fs. The yields of the fragment ions at m/z = 15 (methyl), 43 (acetyl), and 94 (hydroxyphenyl) amu are not shown because they do not change with excitation wavelength and their integrated ion intensity contributes <5% of the overall ion yield for all isomers.

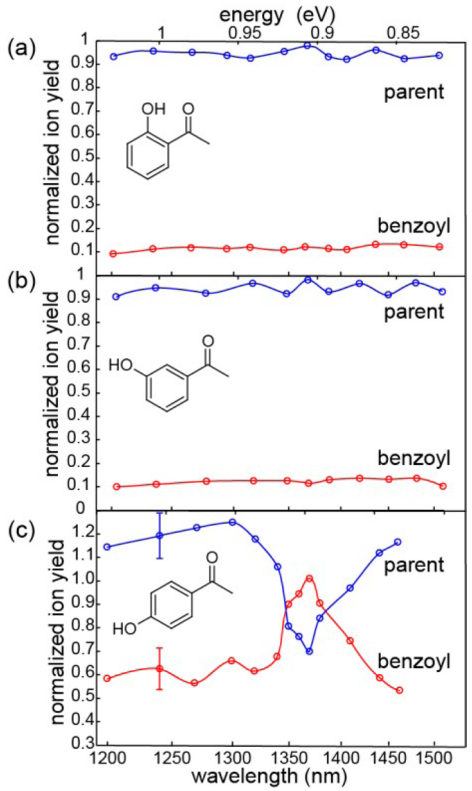

Figure 3. Mass spectral response for 2′- (a), 3′- (b), and 4′- (c) hydroxyacetophenone. All ion yields are normalized to the largest peak in their respective mass spectra at 1370 nm. The laser intensity and pulse duration are maintained at ~5.5 × 10^{13} W cm^{-2} and 65 fs, respectively, across the tuning range. The error bars at 1240 nm in panel c reflect the measured error in the ion yields and are typical for all experiments in this work.

The lack of a dependence on excitation wavelength for the lower mass ions is consistent with previous experiments on acetophenone.[11] The ion yields of the parent and benzoyl ions for 2′- and 3′-hydroxyacetophenone are insensitive to the excitation wavelength across the entire tuning range, with the parent molecular ion accounting for >80% of the total ion yield, approximately 10 times greater than the benzoyl ion yield. Figure 3c reveals that the parent and benzoyl ion yields of 4′-hydroxyacetophenone remain unaffected at excitation wavelengths shorter than 1300 nm. As the wavelength increases above 1300 nm, the parent ion yield decreases and the benzoyl ion yield increases, reaching the minimum parent and maximum benzoyl ion yield at 1370 nm. At longer wavelengths, the parent and benzoyl ion yields return to similar values seen at 1200 nm. The similarity of the fragmentation yield versus excitation wavelength for 4′-hydroxyacetophenone with that for acetophenone and some of its derivatives[11,12] suggests that the photodissociation mechanism may be similar.

To determine the dependence of the parent and benzoyl ion yields on the duration of the excitation pulse, we measured the wavelength-resolved mass spectra for 2′- and 4′-hydroxyacetophenone using a pulse duration of 110 fs, again with a peak intensity of 5.5 × 10^{13} W cm^{-2}. The linear dependence of the ion yields on laser intensity (cf. Figure 2) at a fixed pulse duration indicates that the difference in pulse energy between the 110 and 65 fs pulses should not have a significant effect. The mass spectral responses for the two molecules with 110 and 65 fs pulses are shown in Figure 4a,b, respectively. The

dx.doi.org/10.1021/jp500874r | J. Phys. Chem. A XXXX, XXX, XXX–XXX

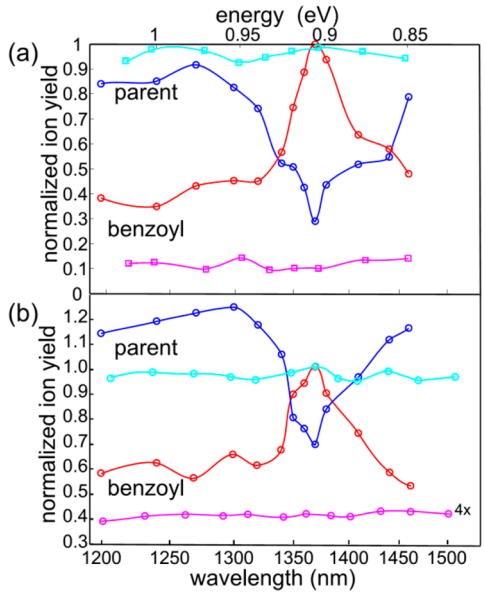

Figure 4. Mass spectral response of 2′- and 4′-hydroxyacetophenone for (a) 110 and (b) 65 fs pulses. The cyan and blue curves correspond to the parent molecular ion in 2′- and 4′-hydroxyacetophenone, respectively, while the magenta and red curves correspond to the benzoyl ion in 2′- and 4′-hydroxyacetophenone, respectively. All spectra are normalized to the largest peak in their mass spectra at 1370 nm.

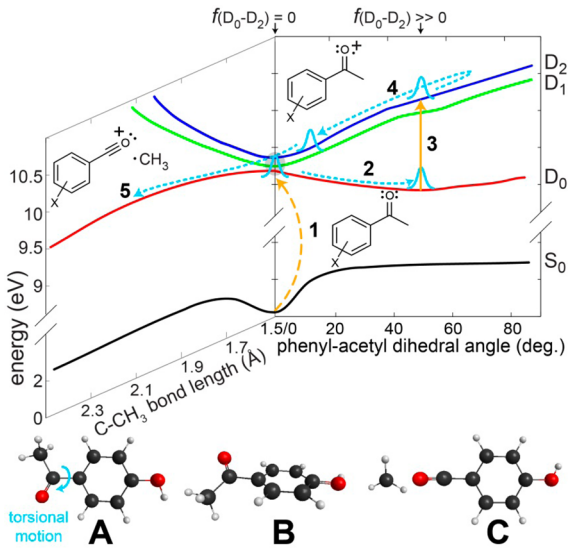

Figure 5. Proposed mechanism for the dissociation of the radical cations of acetophenone and its derivatives. The black, red, green, and blue curves correspond to the S_0, D_0, D_1 and D_2 states, respectively, and were obtained from calculations in ref 11. Structures A–C for 4′-hydroxyacetophenone denote the neutral geometry, optimized ion geometry, and fragmentation products, respectively.

parent and benzoyl ion yields for 2′-hydroxyacetophenone are independent of excitation wavelength for longer pulse duration. In the case of 4′-hydroxyacetophenone, the parent depletion at an excitation wavelength of 1370 nm is approximately four times as strong for 110 fs pulses in comparison with 65 fs pulses. The increased fragmentation yield with longer pulse duration is in accord with previous measurements reported for acetophenone.[13] These results are explained in the Discussion section.

DISCUSSION

The mechanism of parent ion depletion by one-photon absorption upon 1370 nm excitation in the acetophenone radical cation was interpreted using quantum-chemical calculations performed at the MCSCF/cc-pVDZ level of theory.[11] The current understanding of the mechanism for dissociation in acetophenone and its derivatives is summarized in the diagram shown in Figure 5. Tunnel ionization (step 1) creates the parent molecular ion in the neutral geometry (structure A) and launches a torsional wavepacket on the ground state D_0 of the parent molecular ion (step 2), as indicated by the curved arrow around the phenyl-acetyl bond in structure A. At the energy minimum, the molecule has the geometry of structure B and the oscillator strength coupling D_0 to the D_2 surface is nonzero (0.046 in acetophenone), allowing the system to undergo a one-photon resonant transition to the D_2 surface (step 3). The wavepacket proceeds down the D_2 surface toward a conical intersection (step 4), which converts electronic energy to vibrational energy, leading to dissociation along the C–CH_3 bond coordinate (step 5), to form structure C.

Figure 1 reveals that the benzoyl fragment is the principal dissociation product for all hydroxyphenone isomers. Furthermore, in agreement with previous measurements for acetophenone,[11] the dissociation yield increases markedly for 4′-hydroxyacetophenone when the pump wavelength is 1370 nm, indicating a potential resonance. This resonance is confirmed in the plot of the dissociation yield as a function of pump wavelength in Figure 3c. Figure 2 reveals that the yield of both the parent and benzoyl fragment ions increases linearly with peak intensity at all excitation wavelengths, which is consistent with operating beyond the saturation intensity.[14] The linear dependence of the ratio of these ions in 4′-hydroxyacetophenone upon excitation with 1370 nm (not shown) is consistent with measurements on acetophenone[11] and supports the mechanism shown in Figure 5.

We have previously proposed that the time allowed for rotation about the phenyl–carbonyl torsional bond correlates to the amount of dissociation observed.[11] Thus, the dissociation yield should be proportional to the duration of the laser pulse. In this scenario, the peak of the laser pulse will tunnel ionize the molecule, inducing the wavepacket to propagate along the torsional coordinate toward the bright region on the D_0 surface. The latter portion of the pulse excites the system from the D_0 surface to the D_2 surface, leading to subsequent dissociation. In this mechanism, longer duration excitation pulses containing the resonant wavelengths provide the wavepacket with more time to access the bright region and enhance dissociation. This hypothesis was tested by investigating a series of three methyl-substituted acetophenones wherein the reduced moment of inertia about the torsional mode decreased as the methyl substituent was moved from the 2′, or 3′, to the 4′ position with respect to the acetyl group.[12] We observed that the dissociation increased as the reduced moment of inertia decreased. In accord with the torsional motion hypothesis, the decreasing moment of inertia allows more rotation about the torsional axis for a given pulse duration, bringing more of the wavepacket into the bright region for the one photon transition to the D_2 state.

The effect of the position of hydroxyl substitution on the photodissociation of acetophenones is investigated here to

dx.doi.org/10.1021/jp500874r | J. Phys. Chem. A XXXX, XXX, XXX–XXX

further test the effect of torsional motion on the dissociation yield during near-infrared, strong-field excitation. Figures 2 and 4 reveal that the mass spectral response of 4′-hydroxyacetophenone is similar to acetophenone,[11] with an apparent dissociative resonance at 1370 nm producing the benzoyl fragment ion. The presence of the dissociative resonance suggests a mechanism similar to that shown in Figure 5 proposed for acetophenone[11] and its methyl-substituted derivatives.[12] The lack of a feature in the mass spectral responses of 2′- and 3′-hydroxyacetophenone as a function of excitation wavelength shown in Figures 3 and 4 suggests that these isomers do not undergo the mechanism shown in Figure 5.

To explain these results, the neutral and optimized radical cation geometries of the hydroxyacetophenone isomers were calculated at the B3LYP/6-311++G(d,p) level of theory, along with their radical cation ground-state energies, as a function of the phenyl-acetyl dihedral angle. Table 1 summarizes the geometry optimization results, showing the experimental and calculated ionization potentials, the difference in vertical and optimized energy, the difference in O−H bond length for vertical and optimized geometries, adiabatic torsional angles, and reduced moments of inertia. For reference, the values for unsubstituted acetophenone are shown as well. The significant change in length of the O−H bond between the neutral and optimized geometries in 2′-hydroxyacetophenone of 0.047 Å shown in Table 1 suggests that increased hydrogen bonding between the hydroxyl hydrogen and carbonyl oxygen at the optimized geometry restricts the phenyl-acetyl dihedral angle to 0°.

Figure 6 shows the calculated cationic ground-state potential energy surfaces as a function of torsional angle and optimized cationic geometries of each isomer. Figure 6a shows that in 2′-hydroxyacetophenone, a large barrier of 700 meV due to the hydrogen-bonding interaction prevents torsional motion along the phenyl−acetyl dihedral angle coordinate. This barrier limits access to geometries where the D_0-to-D_2 transition dipole is allowed. In principal, adiabatic tunnel ionization imparts little excess energy to the molecular ion and limits the internal energy available for the wavepacket to overcome energy barriers on the surface. Thus, the combination of tunnel ionization and a large potential energy barrier to access a bright geometry explains why no enhanced dissociation to the benzoyl ion is observed in 2′-hydroxyacetophenone.

In the case of 3′-hydroxyacetophenone, calculations reveal that the geometry optimization beginning from coordinates of the neutral geometry converges to the local minimum at a 5° dihedral angle instead of to its global minimum at 150° shown in Figure 6b. We propose that the lack of enhanced dissociation at 1370 nm indicates that the transition to the dissociative excited state is not accessed. The barrier to rotation is 120 meV after vertical excitation of 3′-hydroxyacetophenone. As with the 2′ isomer, this rotational barrier is evidently higher than any excess vibrational energy imparted during tunnel ionization.

The similarities in the excitation wavelength mass spectral responses of 4′-hydroxyacetophenone and acetophenone are presumably due to similar potential energy surfaces,[11] which allow the dissociation process shown in Figure 5 to take place. Both molecules exhibit no barrier to torsional motion when starting from the neutral geometry with a 0° dihedral angle. The global minimum of the 4′-hydroxyacetophenone surface at 35° is not far from the global minimum of the acetophenone surface at 44°. The one-photon transition between the cationic

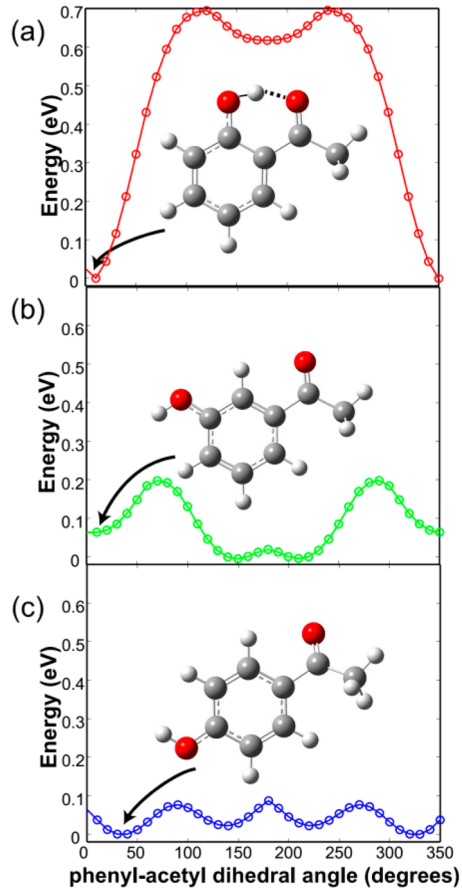

Figure 6. Ground ionic potential-energy surfaces as a function of phenyl-acetyl dihedral angle for 2′- (a), 3′- (b), and 4′- (c) hydroxyacetophenone. The respective optimized geometries for each molecule are included with the black arrow pointing toward the optimized phenyl-acetyl dihedral angle. The surfaces were calculated at the B3LYP/6-311++G(d,p) level of theory.

ground and excited states is symmetry-forbidden at a 0° dihedral angle in acetophenone and increases to 0.046 at 44°[11] The dissociative resonance in 4′-hydroxyacetophenone at 1370 nm suggests that the oscillator strength as a function of dihedral angle is similar to that of acetophenone.

The existence of a rotational barrier in 3′ hydroxyacetophenone, but not in 4′-hydroxyacetophenone, can be explained based on electron delocalization in the respective molecular ions. To visualize the electron charge distributions, we calculated the electron density at the B3LYP/6-311++G(d,p) level of theory, and the electrostatic potential was mapped onto the resulting electron density surface. The electrostatic potential at a given point in space reflects the potential energy of a positive test charge at that location; a negative value denotes a high electron density (i.e., the positive test charge experiences an attractive potential) and a positive value denotes low electron density (i.e., the test charge is repelled).[21] Figure 7a,b shows the mapped electrostatic potentials for the neutrals, ions, and differences between them for 3′- and 4′-hydroxyacetophenone, respectively, with positive electrostatic potential (blue) denoting electron-deficient regions and negative electrostatic potential (red) denoting electron-rich regions. The difference in electrostatic potentials between the neutrals and ions indicates greater electron deficiency on the phenyl ring for both isomers, indicating that ionization removes

dx.doi.org/10.1021/jp500874r | J. Phys. Chem. A XXXX, XXX, XXX−XXX

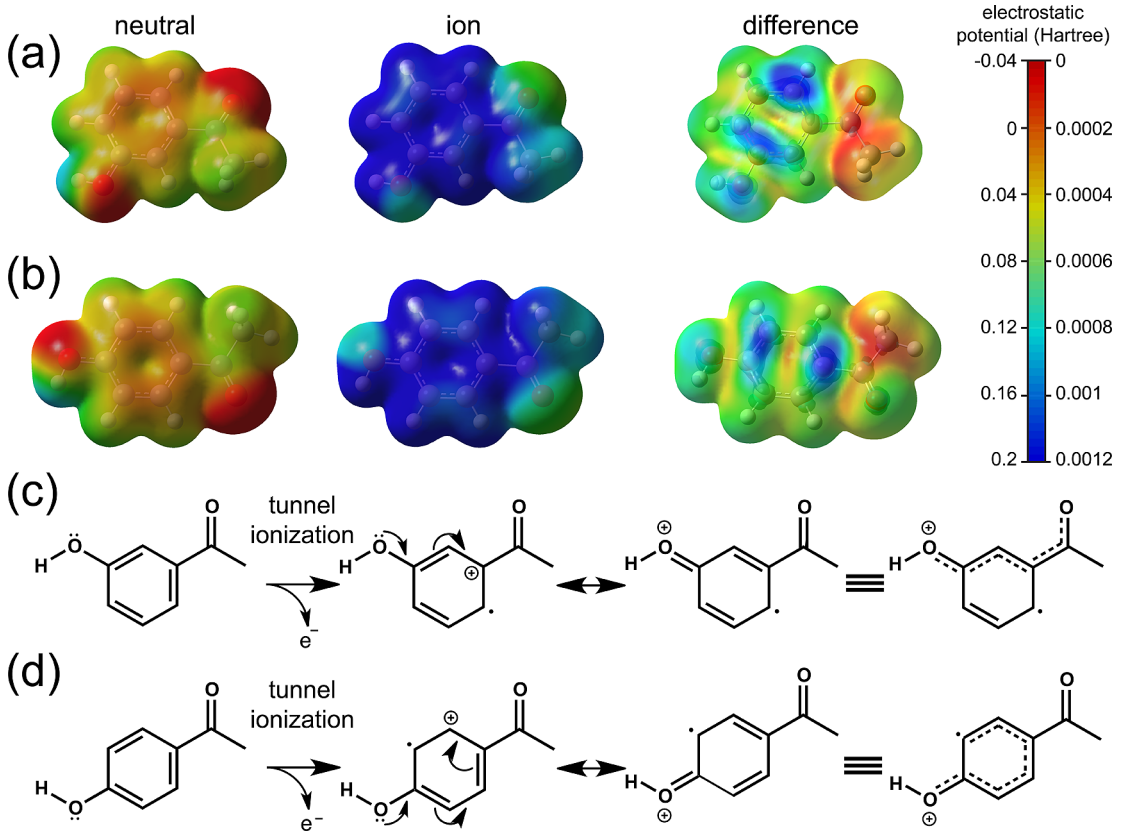

Figure 7. Illustration of charge distributions (a,b) and resonance forms (c,d) contributing to the radical cations of (a,c) 3′-hydroxyacetophenone and (b,d) 4′-hydroxyacetophenone. Electrostatic potentials (Hartree) for the neutral, ion (upon vertical ionization), and difference between them are mapped on a 0.005 e^-/Bohr^3 electron density surface. The numbers on the left-hand side of the scale bar correspond to the electrostatic potentials of the neutral and ion, while the numbers on the right-hand side of the scale bar correspond to the difference. The calculations are performed on B3LYP/6-311++G(d,p) level of theory.

the electron from the phenyl ring. The subsequent electron delocalization is shown by the resonance structures in Figure 7c,d for 3′- and 4′-hydroxyacetophenone, respectively. The local energy minimum at the (nearly) planar geometry in 3′-hydroxyacetophone appears to arise from electron donation by hydroxy group through the electron-deficient phenyl ring to the acetyl group in Figure 7c. This electron delocalization into the acetyl group inhibits rotation away from the planar geometry. In contrast, the analogous resonance forms of 4′-hydroxyacetophenone in Figure 7d do not result in electron delocalization through the acetyl group, so no rotational barrier is expected to arise.

The enhanced dissociation yield in 4′-hydroxyacetophenone at a longer pulse duration (Figure 4) is consistent with previous results for acetophenone.[11] Results of time-resolved pump−probe[22,23] experiments on acetophenone, to be presented in a forthcoming paper,[24] indicate that the period of torsional motion is ∼650 fs, and associated classical wavepacket trajectory calculations[25] based on the ground-state potential energy surface and moment of inertia indicate that the optimal cation torsional angle of 44° is reached after ∼220 fs. For 4′-hydroxyacetophenone, wavepacket trajectory calculations[25] using the potential energy surface in Figure 6c and the moment of inertia in Table 1 suggest that the optimal dihedral angle of 35° is reached in ∼255 fs. The similar time scale required to reach the optimized ionic geometry following tunnel ionization in acetophenone and 4′-hydroxyacetophenone explains their analogous mass spectral responses to changes in pulse duration.

Decreasing the pulse duration from 110 to 65 fs diminishes yield of the benzoyl fragment by a factor of ∼3 at an excitation wavelength of 1370 nm for 4′-hydroxyacetophenone, which is comparable to the factor of ∼4 decrease observed for acetophenone.[11] As previously discussed, the longer pulse duration is expected to more efficiently couple the D_0 and D_2 surfaces because the latter part of the pulse has more temporal overlap with the wavepacket approaching the bright region on the D_0 surface after ∼200 fs. Although the 65 fs pulse does overlap with the wavepacket in the bright region, the shorter temporal overlap results in less of the wavepacket reaching the bright region coupling the D_0 and D_2 surfaces.

■ CONCLUSIONS

Strong field-excitation mass spectrometry from 1200 to 1500 nm for hydroxyacetophenone isomers reveals that the location of substitution on the phenyl ring significantly changes the wavelength-resolved fragmentation response. For 4′-hydroxyacetophenone, a correlated decrease in the parent ion intensity and increase in the benzoyl ion intensity was measured as a function of excitation wavelength in the vicinity of 1370 nm. This response was similar to the resonant dissociation measured previously in unsubstituted acetophenone.[11] DFT calculations using the 6-311++G(d,p) basis set as a function of the phenyl-acetyl dihedral angle revealed no rotational barrier between the neutral and optimal geometry on the ground ionic surface of 4′-hydroxyacetophenone, which enabled the wavepacket to access the bright region. Measurement of the

dx.doi.org/10.1021/jp500874r | J. Phys. Chem. A XXXX, XXX, XXX−XXX

fragmentation yield as a function of pulse duration for 4′-hydroxyacetophenone revealed that a longer pulse interacts with the wavepacket on the D_0 surface for more time than a shorter pulse, thus providing a route to control the amount of the benzoyl ion yield. The lack of wavelength-dependent dissociation in 2′- and 3′-hydroxyacetophenone is attributed to large barriers to rotation about the torsional mode on the ground-state potential energy surfaces, which prevents access to the bright geometry. These results build on the preparation of an electronically cold launch state via tunnel ionization as a tool for examining the electronic properties of radical cations and demonstrate the potential for controlling radical cation dissociation by adding substituent groups.

AUTHOR INFORMATION

Corresponding Author

*E-mail: rjlevis@temple.edu.

Notes

The authors declare no competing financial interest.

ACKNOWLEDGMENTS

We acknowledge the support of the National Science Foundation through grant CHE0957694.

REFERENCES

(1) Hansch, C.; Leo, A.; Hoekman, D. *Exploring QSAR: Fundamentals and Applications in Chemistry and Biology*; American Chemical Society: Washington, DC, 1995.

(2) Bradley, J. C.; Mirza, K.; Lang, A.; Bohinski, T.; Bulger, D.; Merchant, A.; Messner, E.; Moritz, M.; Oseback, S.; Parikh, R.; Shah, M. Open Notebook Science Challenge: Solubilities of Organic Compounds in Organic Solvents. *Nat. Precedings* **2010**, DOI: 10.1038/npre.2010.4243.3.

(3) Neuvonen, H.; Neuvonen, K.; Koch, A.; Kleinpeter, E.; Pasanen, P. Electron-Withdrawing Substituents Decrease the Electrophilicity of the Carbonyl Carbon. An Investigation with the Aid of 13C NMR Chemical Shifts, ν(CO) Frequency Values, Charge Densities, and Isodesmic Reactions To Interprete Substituent Effects on Reactivity. *J. Org. Chem.* **2002**, *67* (20), 6995−7003.

(4) Hansch, C.; Leo, A.; Taft, R. W. A Survey of Hammett Substituent Constants and Resonance and Field Parameters. *Chem. Rev.* **1991**, *91* (2), 165−195.

(5) Yuan, L.; Li, C.; Lin, J. L.; Yang, S. C.; Tzeng, W. B. Mass Analyzed Threshold Ionization Spectroscopy of o-Fluorophenol and o-Methoxyphenol Cations and Influence of the Nature and Relative Location of Substituents. *Chem. Phys.* **2006**, *323* (2−3), 429−438.

(6) Cardoza, D.; Baertschy, M.; Weinacht, T. Understanding Learning Control of Molecular Fragmentation. *Chem. Phys. Lett.* **2005**, *411* (4−6), 311−315.

(7) Bergt, M.; Brixner, T.; Dietl, C.; Kiefer, B.; Gerber, G. Time-Resolved Organometallic Photochemistry: Femtosecond Fragmentation and Adaptive Control of CpFe(CO)2X (X=Cl, Br, I). *J. Organomet. Chem.* **2002**, *661* (1−2), 199−209.

(8) Moore Tibbetts, K.; Xing, X.; Rabitz, H. Systematic Trends in Photonic Reagent Induced Reactions in a Homologous Chemical Family. *J. Phys. Chem. A* **2013**, *117* (34), 8205−8215.

(9) Moore Tibbetts, K.; Xing, X.; Rabitz, H. Optimal Control of Molecular Fragmentation with Homologous Families of Photonic Reagents and Chemical Substrates. *Phys. Chem. Chem. Phys.* **2013**, *15* (41), 18012−18022.

(10) Moore Tibbetts, K.; Xing, X.; Rabitz, H. Exploring Control Landscapes for Laser-Driven Molecular Fragmentation. *J. Chem. Phys.* **2013**, *139* (14), 144201.

(11) Bohinski, T.; Moore Tibbetts, K.; Tarazkar, M.; Romanov, D.; Matsika, S.; Levis, R. Measurement of Ionic Resonances in Alkyl Phenyl Ketone Cations via Infrared Strong Field Mass Spectrometry. *J. Phys. Chem. A* **2013**, *117* (47), 12374−12381.

(12) Bohinski, T.; Moore Tibbetts, K.; Tarazkar, M.; Romanov, D.; Matsika, S.; Levis, R. Radical Cation Spectroscopy via Tunnel Ionization. *Chem. Phys.* **2014**, submitted.

(13) Bohinski, T.; Moore Tibbetts, K.; Tarazkar, M.; Romanov, D.; Matsika, S.; Levis, R. J. Measurement of an Electronic Resonance in a Ground-State, Gas-Phase Acetophenone Cation via Strong-Field Mass Spectrometry. *J. Phys. Chem. Lett.* **2013**, *4*, 1587−1591.

(14) Hankin, S. M.; Villeneuve, D. M.; Corkum, P. B.; Rayner, D. M. Intense-Field Laser Ionization Rates in Atoms and Molecules. *Phys. Rev. A: At. Mol. Opt. Phys.* **2001**, *64* (1), 013405.

(15) Frisch, M.; Trucks, G.; Schlegel, H.; Scuseria, G.; Robb, M.; Cheeseman, J.; Scalmani, G.; Barone, V.; Mennucci, B.; Petersson, G. *Gaussian 09*, revision B. 01; Gaussian, Inc.: Wallingford, CT, 2010.

(16) Cramer, C. J. *Essentials of Computational Chemistry: Theories and Models*; John Wiley & Sons: Hoboken, NJ, 2013.

(17) Burke, K. Perspective on Density Functional Theory. *J. Chem. Phys.* **2012**, *136* (15), 150901.

(18) Kobayashi, T.; Nagakura, S. Photoelectron Spectra of Substituted Benzenes. *Bull. Chem. Soc. Jpn.* **1974**, *47* (10), 2563−2572.

(19) Foffani, A.; Cantone, B.; Pignataro, S.; Grasso, F. Ionization Potentials and Substituent Effects for Aromatic Carbonyl Compounds. *Z. Phys. Chem. (Frankfurt)* **1964**, *42* (3−4), 221−235.

(20) Pignatar., S.; Foffani, A.; Innorta, G.; Distefan, G. Molecular Structural Effects on the Ionization Potentials for Meta Substituted Aromatic Compounds and for Compounds of the Type X-CH2-R. *Z. Phys. Chem. (Frankfurt)* **1966**, *49* (6), 291−298.

(21) Mecozzi, S.; West, A. P.; Dougherty, D. A. Cation-pi Interactions in Aromatics of Biological and Medicinal Interest: Electrostatic Potential Surfaces as a Useful Qualitative Guide. *Proc. Natl. Acad. Sci.* **1996**, *93* (20), 10566−10571.

(22) Geißler, D.; Rozgonyi, T.; González-Vázquez, J.; González, L.; Marquetand, P.; Weinacht, T. C. Pulse-Shape-Dependent Strong-Field Ionization Viewed with Velocity-Map Imaging. *Phys. Rev. A* **2011**, *84* (5), 053422.

(23) Geißler, D.; Marquetand, P.; González-Vázquez, J.; González, L.; Rozgonyi, T.; Weinacht, T. Control of Nuclear Dynamics with Strong Ultrashort Laser Pulses. *J. Phys. Chem. A* **2012**, *116* (46), 11434−11440.

(24) Bohinski, T.; Moore Tibbetts, K.; Tarazkar, M.; Romanov, D. A.; Matsika, S.; Levis, R. J. Time Resolved Dynamics of Acetophenone Radical Cation. **2014**, in preparation.

(25) Rose, T. S.; Rosker, M. J.; Zewail, A. H. Femtosecond Real-Time Observation of Wave Packet Oscillations (Resonance) in Dissociation Reactions. *J. Chem. Phys.* **1988**, *88* (10), 6672−6673.